C. R. Chimie 15 (2012) 229–236

Contents lists available at SciVerse ScienceDirect

Comptes Rendus Chimie

www.sciencedirect.com

Full paper/Mémoire

Intramolecular d^{10}–d^{10} interactions in neutral, dinuclear Au(I) complexes supported by amino-thiazoline- and -thiazole-based P,N-phosphine ligands

Corinna Voß, Roberto Pattacini, Pierre Braunstein *

Laboratoire de chimie de coordination, UMR 7177 CNRS, université de Strasbourg, institut Le Bel, 4, rue Blaise-Pascal, CS 90032, 67081 Strasbourg cedex, France

ARTICLE INFO

Article history:
Received 23 August 2011
Accepted after revision 21 September 2011
Available online 24 October 2011

Dedicated to the memory of our friend and colleague Marie-adeleine Rohmer.

Keywords:
Coordination chemistry
Gold chemistry
Metallophilic interactions
Assembling ligands
P,N ligands
Crystal structures
Dinuclear complexes

ABSTRACT

The ligands *N*-(diphenylphosphino)-thiazoline-2-amine (**1**), *N*-(diphenylphosphino)thiazol-2-amine (**2**) and *N*-(diphenylphosphino)-1,3,4-thiadiazol-2-amine **3**, readily reacted with [AuCl(THT)] in dichloromethane to form the linearly coordinated complexes [AuCl(**1**-κ*P*)] (**5**), [AuCl(**2**-κ*P*)] (**6**) and [AuCl(**3**-κ*P*)] (**7**), respectively. Facile deprotonation with *t*-BuOK or Na_2CO_3 of **5–7** afforded the stable, *neutral* dinuclear complexes [AuCl(**1**$_{-H}$-κ*P*,κ*N*)]$_2$ (**8**), [AuCl(**2**$_{-H}$-κ*P*,κ*N*)]$_2$ (**9**) and [AuCl(**3**$_{-H}$-κ*P*,κ*N*)]$_2$ (**10**), respectively. The crystal structures of the mononuclear complexes **5**, **6** and **7** and of the dinuclear complexes **8**, **9** and **10** have been determined by X-ray diffraction. The latter represent rare examples of neutral complexes supported by bridging P,N-ligands which display intramolecular Au(I)···Au(I) d^{10}–d^{10} interactions, in the range 2.8592(4)–2.8831(4) Å.

1. Introduction

It is now well established that Au(I) centres are prone to display d^{10}–d^{10} metal–metal interactions [1]. The term "aurophilicity" is commonly used to refer to such interactions in the structural chemistry of gold complexes. Although positively charged Au^I ($[Xe]4f^{14}5d^{10}$) ions could be expected to repel each other on the basis of electrostatics, the attractive interactions between these closed valence shell ions result in interatomic distances typically in the range between 2.7 and 3.3 Å, often shorter than the sum of the van der Waals radii [1]. This phenomenon could not be explained by conventional descriptions of chemical bonding [2], but is now well described as dispersion-driven and enhanced by relativistic effects [1,2]. However, the conditions for the occurrence of aurophilicity and its structural, physical and chemical consequences remain difficult to predict, hence further experimental and theoretical studies on d^{10}–d^{10} interactions are needed, whether in homo- or in heterometallic systems [1–3]. One way to promote the generation of Au(I)–Au(I) interactions is to use assembling ligands to stabilize dinuclear complexes, the simplest candidates for such a bonding type. Slight modifications in the structural and/or electronic properties of the assembling ligand could allow a fine-tuning of the metal–metal bond length. Thus, we selected the phosphinoaminothiazoles reported in Scheme 1, namely *N*-(diphenylphosphino)-thiazoline-2-amine (**1**) [4], *N*-(diphenylphosphino)thiazol-2-amine (**2**) [5,6], *N*-(diphenylphosphino)benzo[*d*]thiazol-2-amine (**3**) [5], *N*-(diphenylphosphino)-1,3,4-thiadiazol-2-amine (**4**) [5], which readily form 5-membered ring chelates with, e.g., d^8-metal ions, as potential bridging ligands in gold chemistry for the generation of d^{10}–d^{10} interactions because of their stereoelectronic features, the commercial availability of their precursors and their

* Corresponding author.
E-mail address: braunstein@unistra.fr (P. Braunstein).

1631-0748/$ – see front matter © 2011 Académie des sciences. Published by Elsevier Masson SAS. All rights reserved.
doi:10.1016/j.crci.2011.09.010

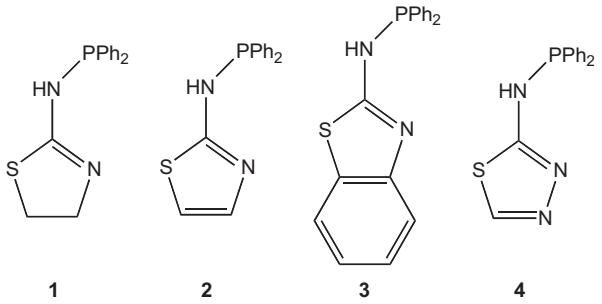

Scheme 1.

stability when deprotonated [4,5]. Owing to their good bridging properties, we have recently used the deprotonated ligands $\mathbf{1}_{-H}$ and $\mathbf{4}_{-H}$ for the formation of, respectively, heterobimetallic coordination polymers and complexes, utilizing the free P-bound N donor [7], or homo- and heterobimetallic complexes, the latter by taking advantage of the endo-cyclic N = CH nitrogen [8]. The complex [Pt($\mathbf{1}_{-H}$-κ*P*,κ*N*)$_2$] showed interesting vapoluminescent properties, its emission in the visible region, when excited by UV radiation, being dramatically enhanced upon exposure to alcohols [5]. The non-coordinated N function of the latter complex is also reactive towards organic nucleophiles, e.g. leading to the formation of [Pt($\mathbf{1}_{-H}$-κ*P*,κ*N*)($\mathbf{1}_{-H}$·EtNCS-κ*P*,κ*S*] by reaction with EtN = C = S [7]. We expected that deprotonated ligands $\mathbf{1}_{-H}$ – $\mathbf{4}_{-H}$ could form stable dinuclear gold complexes displaying Au···Au interactions, efficiently supported by a P–N bridging mode of these heteroditopic ligands.

2. Experimental

2.1. General considerations

All manipulations were carried out under inert atmosphere, using standard Schlenk-line techniques and dried and freshly distilled solvents. The ^{1}H, ^{13}C{^{1}H}, and ^{31}P{^{1}H} NMR spectra were recorded at 298 K by using the instruments Bruker Avance 300 at 300.13, 75.47 and 121.49 MHz, respectively, or Bruker Avance 400 at 400.13, 100.61, 161.98 MHz and Bruker Avance 500 at 500.13, 125.76, 202.46 MHz, respectively, using TMS or H_3PO_4 (85% in D_2O) as external standard with downfield shifts reported as positive. All spectra were measured at 298 K. The assignments of the signals were made by ^{1}H, ^{1}H-COSY, ^{1}H, ^{13}C-HMBC and ^{1}H, ^{13}C, HMQC experiments. Elemental C, H, N and S analyses were performed by the "Service central d'analyses", *Centre national de la recherche scientifique*, Lyon or by the "Service de microanalyses", *université de Strasbourg*. IR spectra were recorded in the region 4000–150 cm^{-1} on a Nicolet 6700 FTIR equipped with the ATR accessory Smart Orbit with diamond crystal. The following compounds were prepared according to literature procedures: [AuCl(THT)] [9], **1** [4] **2** and **3** [5]. PPh_2Cl was freshly distilled before use. Other chemicals were commercially available and used as received.

2.2. Synthesis of [AuCl(**1**-κ*P*)] (**5**)

Solid ligand **1** (0.300 g, 1.05 mmol) was dissolved in dichloromethane (50 mL) and [AuCl(THT)] (0.340 g, 1.06 mmol) was added. This solution was stirred under N_2 at room temperature for 1 h. The volatiles were removed under reduced pressure. A colourless powder was obtained and washed twice with 20 mL of diethylether, giving **5**. The precipitate was collected by filtration and dried under vacuum. Yield: 0.523 g (96% based on ligand **1**). Elemental analysis (%) calcd for $C_{15}H_{15}AuClN_2PS$; *M* = 518.75: C, 34.73; H, 2.91; N, 5.40. Found: C, 34.74; H, 3.15; N, 5.46. ^{1}H NMR ($CDCl_3$, 300 MHz) [ppm]: δ = 7.73 (m, 4H, *o*-phenyl), 7.42–7.39 (m, 6H, *m,p*-phenyl), 6.25 (s, br, 1H, NH), 3.63 (t, ^{3}J(H,H) = 7.2 Hz, 2H, CH_2-N) and 3.41 (t, ^{3}J(H,H) = 7.2 Hz, 2H, CH_2-S). The poor solubility of (**5**) in common organic solvents prevented the recording of a good quality ^{13}C NMR spectrum. ^{31}P{H} NMR ($CDCl_3$, 121 MHz) [ppm]: δ = 60.8. FTIR (solid, cm^{-1}): 1599 [s, ν(C = N)], Far-IR (solid, cm^{-1}): ν = 320 [s, ν(AuCl)].

2.3. Synthesis of [AuCl(**2**-κ*P*)] (**6**)

Solid ligand **2** (0.100 g, 0.35 mmol) was dissolved in dry dichloromethane (15 mL) and solid [AuCl(THT)] (0.113 g, 0.35 mmol) was added to the solution. This mixture was stirred under N_2 for 1 h. The solvent was evaporated under reduced pressure. Complex **6** was obtained as a colourless solid, washed twice with diethyl ether (5 mL) and dried under vacuum. Single crystals suitable for X-ray analysis were obtained by layering a CH_2Cl_2 solution with pentane. Yield: 0.128 g (71% based on ligand **2**). Elemental analysis (%) calcd for $C_{15}H_{13}AuClN_2PS$; *M* = 516.74: C, 34.87; H, 2.54; N, 5.42 Found: C, 34.39; H, 2.69; N, 5.34. ^{1}H NMR ($CDCl_3$, 300 MHz) [ppm]: δ = 7.73 (ddd, 4H, ^{3}J(PH) = 14 Hz, ^{3}J(HH) = 7.1 Hz, ^{4}J(HH) = 1.9 Hz; *o*-Ph), 7.4–7.6 (m, 6H; *m,p*-Ph), 6.19 (dd, ^{3}J(H,H) = 4.5 Hz, ^{5}J(P,H) = 1.5 Hz, 1H; N-CH), 5.88 (dd, ^{3}J(H,H) = 4.5 Hz, ^{5}J(P,H) = 3.3 Hz, 1H; S-CH). ^{13}C{H} NMR ($CDCl_3$, 300 MHz) [ppm]: δ = 169.9 (s, N-C = N), 132.5 (d, partly masked; *i*-phenyl) 132.5 (d, ^{2}J(C,P) = 15 Hz; *o*-Ph), 132.2 (s; *p*-Ph), 129.1, (d, ^{3}J(C,P) = 12 Hz; *m*-phenyl), 129.17 (d, *J* = 14 Hz; *i*-Ph), 125.7 (s; S–CH = C), 107.3 (s; N–CH = C). ^{31}P{H} NMR ($CDCl_3$, 121 MHz) [ppm]: δ = 60.2. FTIR (solid, cm^{-1}): 1580 [s, ν(C = N)]. Far-IR (solid, cm^{-1}): 321 [s, ν(Au–Cl)].

2.4. Synthesis of [AuCl(**3**-κ*P*)] (**7**)

Solid [AuCl(THT)] (0.150 g, 0.47 mmol) was dissolved in dichloromethane (20 mL) and a solution of ligand **3** (0.157 g, 0.47 mmol) in dichloromethane (20 mL) was added. The mixture was stirred under N_2 for 1 h. The volatiles were removed under reduced pressure. A colourless precipitate was obtained. The solid was washed three times with 20 mL diethylether and dried under vacuum to give complex **7** which was recrystallized by layering pentane on a saturated $CHCl_3$ solution. Yield: 0.126 g (48% based on [AuCl(THT)]). Elemental analysis (%) calcd for $C_{19}H_{15}AuClN_2PS$; *M* = 566.79: C, 40.26; H, 2.67; N, 4.94; S, 5.66. Found: C, 39.91; H, 2.79; N, 4.81; S, 5.63. ^{1}H NMR ($CDCl_3$, 300 MHz) [ppm]: δ = 7.78 (ddd, 4H,

^3J(P,H) = 13.9 Hz, ^3J(H,H) = 7.5 Hz, ^4J(H,H) = 1.7 Hz; *o*-phenyl), 7.50–7.38 (m, 7H; *p,m*-phenyl, H4), 7.29 (m, 1H; H6) 7.15 (m, 2H; H7 and H5). ^{13}C{H} NMR: 167.0 (d, ^2J(C,P) = 6.8 Hz; C = N), 137.40 (s; benzo), 136.4 (s; benzo), 133.5 (d, ^1J(C,P) = 75 Hz; *i*-phenyl), 132.3 (d, ^2J(C,P) = 15.0 Hz; *o*-phenyl), 131.8 (s, *p*-phenyl), 128.9 (d, ^3J(C,P) = 12.5 Hz; *m*-phenyl), 127.1 (s; C6), 123.7 (s; C5), 122.7 (s; C4), 111.8 (s; C7). ^{31}P{H} NMR ($CDCl_3$, 121 MHz) [ppm]: δ = 59.5. FTIR (solid, cm^{-1}): 1564 [s, ν(C = N)], Far-IR (solid, cm^{-1}): 319 [s, ν(AuCl)].

2.5. Synthesis of [Au(**1**$_{-H}$-κ*P*,κ*N*)]$_2$ (**8**)

Solid complex **5** (0.414 g, 0.80 mmol) was dissolved in dichloromethane (30 mL) and *t*-BuOK (0.300 g, 26 mmol) was added. The solution was stirred under N_2 at room temperature for 1 h. The suspension was filtered and the solution was evaporated under reduced pressure. The solid was dissolved in 20 mL dichloromethane and pentane was added. Colourless **8** precipitated and was collected by decantation. Yield: 0.254 g (68% based on complex **5**. Elemental analysis (%) calcd for $C_{30}H_{28}Au_2N_4P_2S_2$; *M* = 964.58: C, 37.36; H, 2.93; N, 5.81. Found: C, 37.53; H, 2.97; N, 5.73. ^{1}H NMR ($CDCl_3$; 300 MHz) [ppm]: δ = 7.53 (m, 8H; *o*-phenyl), 7.34–7.22 (m, 12H; *m,p*-phenyl), 4.20 (t, ^3J(H,H) = 7.2 Hz, 4H; NCH_2), 3.28 (t, ^3J(H,H) = 7.2 Hz, 4H; SCH_2). ^{13}C{^{1}H} NMR ($CDCl_3$; 100 MHz) [ppm]: δ = 175.7 (s; N–C–N), 138.0 (d, ^1J(C,P) = 75 Hz), 131.7 (“filled-in” d, simulated, ^{2+5}J(C,P) ≈ 14 Hz, ^3J(P,P) ≈ 9.5 Hz; *o*-Ph), 130.4 (s; *p*-Ph), 128.6 (“filled-in” d, simulated, ^{3+6}J(C,P) ≈ 12 Hz, ^3J(P, P) ≈ 9.5 Hz; *m*-Ph), 59.73 (N–CH_2), 32.16 (S–CH_2). ^{31}P{H} NMR ($CDCl_3$; 121 MHz) [ppm]: δ = 42.0. FTIR (solid, cm^{-1}): 1560 [s, ν(C = N)].

2.6. Synthesis of [Au(**2**$_{-H}$-κ*P*,κ*N*)]$_2$ (**9**)

Solid complex **6** (0.088 g, 0.17 mmol) was dissolved in dichloromethane (25 mL) and *t*-BuOK (0.037 g, 0.32 mmol) was added under N_2 and the solution was stirred for 1 h. The mixture was filtered and the solvent was evaporated under reduced pressure. A colourless precipitate of **9** was formed, collected and washed with Et_2O (30 mL). This dinuclear complex was recrystallized by layering pentane on a saturated dichloromethane solution. Yield: 0.031 g (19% based on complex **6**). Elemental analysis (%) calcd for $C_{30}H_{24}Au_2N_4P_2S_2$; *M* = 960.55: C, 37.51; H, 2.52; N, 5.83. Found: C, 36.80; H, 2.88; N, 5.64. ^{1}H NMR ($CDCl_3$; 300 MHz) [ppm]: δ = 7.56 (m, 8H; *o*-Ph), 7.35–7.20 (m, 12H; *m,p*-Ph), 6.94 (d, 1H, ^3J = 4.5 Hz; N–CH), 6.26 (dd, ^3J(H,H) = 4.5 Hz, ^5J(H,P) = 5 Hz, 1H; S–CH). The poor solubility of compound **9** in common organic solvents prevented the recording of the ^{13}C spectrum. ^{31}P{H} NMR ($CDCl_3$; 121 MHz) [ppm]: δ = 39.0. FTIR (solid, cm^{-1}): 1574 [s, ν(C = N)].

2.7. Synthesis of [Au(**3**$_{-H}$-κ*P*,κ*N*)]$_2$ (**10**)

Solid [AuCl(THT)] (0.200 g, 0.62 mmol) and ligand **3** (0.207 g, 0.62 mmol) were dissolved in dichloromethane (50 mL). The reaction mixture was stirred under N_2 for 1 h. Sodium carbonate (0.700 g, 6.60 mmol) was added and the mixture was stirred for 5 h. The solid was filtered off and the filtrate taken to dryness under reduced pressure, affording a colourless precipitate. It was washed twice with 20 mL diethylether, giving **10**. Yield: 0.196 g (60% based on ligand **3**. Complex **10** was crystallized by layering pentane on a saturated $CHCl_3$ solution. Elemental analysis (%) calcd for $C_{38}H_{28}Au_2N_4P_2S_2$; *M* = 1060.67: C, 43.03; H, 2.66; N, 5.28. Found: C, 42.95; H, 2.78; N, 5.14. ^{1}H NMR ($CDCl_3$; 500 MHz) [ppm]: δ = 7.68–7.60 (m, 10H; *o*-phenyl and H7), 7.43 (dd, 2H, ^3J(H,H) = 7.5 Hz, ^4J(H,H) = 1.5 Hz; H4), 7.38 (m, 4H; *p*-phenyl), 7.32 (m, 8H; *m*-phenyl), 7.15 (ddd, ^3J(H,H) = 7.5 Hz, ^3J(H,H) = 7.7 Hz, ^4J(H,H) = 1.0 Hz; H6), 7.07 (ddd, ^3J(H,H4) = ^3J(H,H5) = 7.5 Hz, ^4J(H,H) = 1.5 Hz; H5); ^{13}C{H} NMR ($CDCl_3$; 125 MHz) [ppm]: δ = 174.9 (s, N–C = N), 149.4 (s; C3) 137.3 (d, ^1J(C,P) = 61 Hz; *i*-Ph), 131.3 (“filled-in” d, simulated, ^{2+5}J(C,P) ≈ 17 Hz, ^3J(P,P) ≈ 12 Hz; *o*-Ph), 130.5 (s; *p*-Ph), 128.7 (“filled-in” d, simulated, ^{3+6}J(C,P) ≈ 10 Hz, ^3J(P,P) ≈ 12 Hz; *m*-Ph), 128.7 (dd, ^4J(P,C) = 3 Hz, ^4J(P,C) = 3 Hz; C2), 125.2 (s; C6), 122.3 (s; C5), 120.8 (s; C4), 116.7 (s; C7). ^{31}P{H} NMR ($CDCl_3$; 121 MHz) [ppm]: δ = 39.5. FTIR (solid, cm^{-1}): 1565 [s, ν(C = N)].

2.8. X-ray data collection and refinement for **5–10**

Suitable crystals for the X-ray analysis were obtained as described above. The intensity data were collected at 173(2) K on a Kappa CCD diffractometer [10] (graphite monochromated Mo-Kα radiation λ = 0.71073 Å). The structures were solved by direct methods (SHELXS-97) and refined by full-matrix least-squares procedures (based on F^2, SHELXL-97) [11] with anisotropic thermal parameters for all the non-hydrogen atoms. The hydrogen atoms were introduced into the geometrically calculated positions (SHELXL-97 procedures) and refined riding on the corresponding parent atoms, except those on N atoms which were found in the difference maps and refined isotropically. Data collection and refinement parameters for **5–10** are reported in Table 1. CCDC 840772–840777 (**5–10**) contain the supplementary crystallographic data for this paper that can be obtained free of charge from the Cambridge Crystallographic Data Centre via www.ccdc cam.ac.uk/data_request/cif.

3. Results and discussion

The colourless complex **5** was prepared by reaction of ligand **1** with [AuCl(THT)] (tetrahydrothiophene [THT]) in dichloromethane, at room temperature for 1 h (Scheme 1).

The NH proton has been displayed on the exo-cyclic nitrogen in **1**, **2** and **3** for clarity, but the other tautomer with the H atom on the endo-cyclic nitrogen is also present in solution for **1** (Scheme 2).

The crystal structure of complex **5** was determined by single crystal X-ray diffraction and is shown in Fig. 1.

In the crystal structure of complex **5** (Fig. 1), ligand **1** coordinates to the gold atom through the phosphorus atom. A terminal chloride also coordinates the metal centre, that adopts an almost linear coordination geometry [Cl1–Au1–P1 177.95(4)]. The NH proton has been found in the difference map and could be located on the endo-cyclic N atom. Centrosymmetric pairs of complexes are connected through two N–H···N hydrogen bonds, between the

Table 1
X-ray data collection and refinement parameters for **5–10**.

Compound	**5**	**6**	**7**	**8**	**9**	**10**
Formula	$C_{15}H_{15}Au_1Cl_1N_2PS$	$C_{15}H_{13}AuClN_2PS$	$C_{19}H_{15}AuClN_2PS$	$C_{30}H_{28}Au_2N_4P_2S_2$	$C_{30}H_{24}Au_2N_4P_2S_2$	$C_{38}H_{28}Au_2N_4P_2S_2$
Mass	518.74	516.72	566.79	964.56	960.53	1060.64
Crystal system	Triclinic	Monoclinic	Monoclinic	Orthorhombic	Monoclinic	Triclinic
a/Å	8.5661(3)	12.7527(6)	11.9973(7)	9.1049(3)	16.4751(6)	12.2324(4)
b/Å	8.8903(3)	8.6138(5)	10.1616(3)	23.3032(8)	11.3575(6)	17.0012(5)
c/Å	11.300(5)	18.7048(8)	18.9570(8)	28.4310(11)	18.0291(7)	18.3825(5)
α/°	90.216(10)	90.00	90.00	90.00	90.00	77.8494(16)
β/°	103.867(10)	129.342(3)	125.438(3)	90.00	120.607(3)	72.2786(15)
γ/°	101.928(3)	90.00	90.00	90.00	90.00	70.3212(15)
V/Å^3	816.11(5)	1589.06(14)	1882.94(15)	6032.3(4)	2903.5(2)	3403.9(2)
T/K	173(2)	173(2)	173(2)	173(2)	173(2)	173(2)
Space group	*P*-1	*P*21/*c*	*P*21/*c*	*F*2*dd*	*P*21/*c*	*P*-1
Z	2	4	4	8	4	4
μ/mm^{-1}	9.396	9.651	8.155	9.990	10.377	8.863
No. of meads. refl.	5244	5895	9675	6097	1,1211	2,2599
No. of indep. refl.	3937	3621	5486	3236	6906	15530
R_{int}	0.0304	0.0380	0.0373	0.0490	0.0570	0.0304
R_1 ($I > 2\sigma(I)$)	0.0309	0.0408	0.0359	0.0461	0.0445	0.0406
$wR(F^2)$ ($I > 2\sigma(I)$)	0.0625	0.0923	0.0774	0.1130	0.0671	0.0941
R_1 (all data)	0.0415	0.0746	0.0736	0.0516	0.0936	0.0838
$wR(F^2)$ (all data)	0.0652	0.1282	0.1097	0.1164	0.0787	0.1346
S on F^2	1.031	1.078	1.016	1.033	0.964	1.025
Flack parameter			0.015(14)			

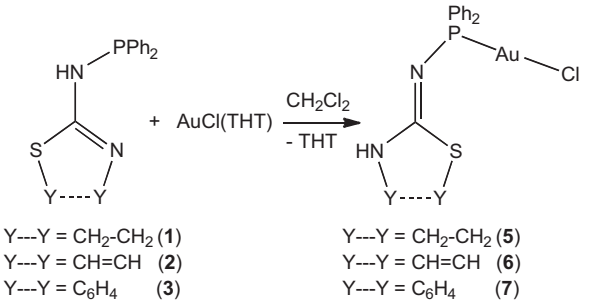

Scheme 2.

exo-cyclic (acceptor) and the endo-cyclic (donor) nitrogen atoms, as shown is Fig. 2 (N···N distance between opposite atoms: 3.124(5) Å), to form pseudo-dimers.

The bonding parameters in **5** are consistent with those in other P–Au–Cl complexes, such as [AuCl(PPh_3)] [12] (P–Au–Cl 177.95(4)°, P–Au 2.235(3) Å and Au–Cl 2.288(1) Å).

The spectroscopic data in solution are consistent with the solid-state structure. The $^{31}P\{^1H\}$ NMR spectrum consists of a singlet at 60.8 ppm, downfield shifted with respect to the free ligand (49 ppm) [4]. Complex **5** exhibits in the IR spectrum a very intense ν(Au–Cl) stretching absorption at 320 cm^{-1} which is comparable to that of [AuCl(THT)] [9] (332 cm^{-1}) and of [AuCl(SMe_2)] [13] (325 cm^{-1}). The NH proton gives rise to a broad signal at 6.25 ppm.

A similar reaction was performed with *N*-(diphenylphosphino)thiazol-2-amine (ligand **2**) instead of **1** and gave [AuCl(**2**)] (**6**). Its crystal structure is shown in Fig. 3.

The Au(I) atom is coordinated by the phosphorus donor of ligand **2** and by a terminal chloride. As in **5**, the coordination geometry is almost linear (177.7(1)°) and the bond lengths are similar to those in **5**. As a result of the aromaticity of the thiazole ring, the endo-cyclic bond distances are significantly shorter than those in **1**. The NH proton has been found in the difference maps and is located on the endo-cyclic nitrogen, as in **5**. Hydrogen bonded pseudo-dimers, similar to those encountered in **5** are also observed in the case of **6**, although a shorter N···N separation was observed, 2.93(1) Å *vs.* 3.124(5) Å in **5**. This is likely due to the absence of methylene protons in **6**, that

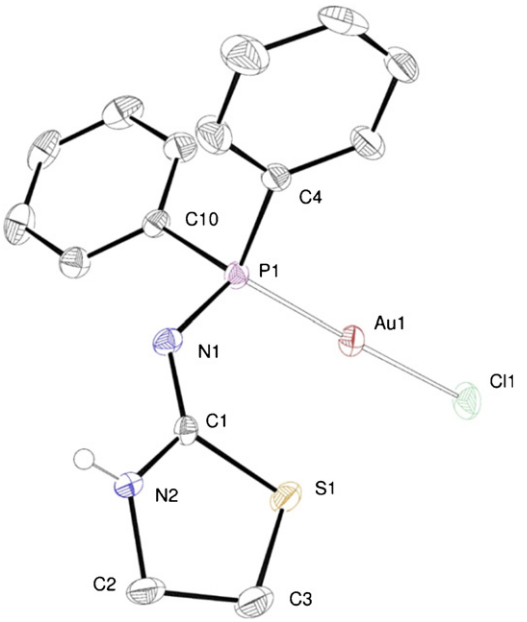

Fig. 1. ORTEP of the molecular structure of complex **5**. Ellipsoids at 40% probability level. Selected bond lengths [Å] and angles [°]: Au1–Cl(1) 2.288(1), Au1–P1 2.227(1), P1–N1 1.661(4), N1–C1 1.312(6), N1–C1 1.312(6), C1–N2 1.310(7), N2–C2 1.460(7), C2–C3 1.505(8), C3–S1 1.814(6), S1–C1 1.784(4); Cl1–Au1–P1 177.95(4), Au1–P1–N1 118.5(1), P1–N1–C1 124.9(3), N1–C1–N2 123.3(4), N1–C1–S1 126.4(3), N2–C1–S1 110.2(3).

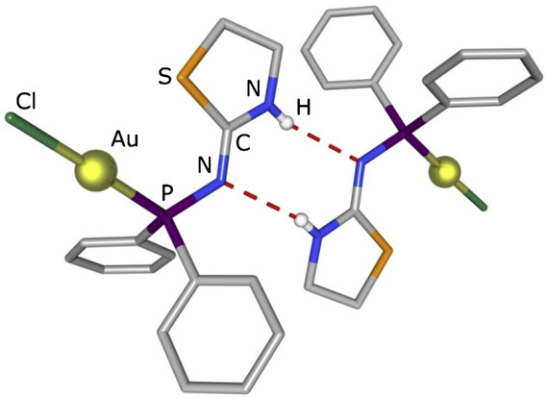

Fig. 2. Diagram of the crystal structure of **5**, showing a pair of complex molecules connected by N–H···N hydrogen bonds (symmetry operation generating equivalent atoms: –x, –y, –z).

exert steric hindrance towards the phenyls of the centrosymmetric counterpart in **5**.

The $^{31}P\{^{1}H\}$ NMR spectrum of **6** is similar to that of **5**, and consists in a singlet centered at 60.2 ppm. The solid state FTIR spectrum shows the diagnostic ν(Au–Cl) band at 321 cm^{-1}. The N–CH and S–CH protons of the thiazole ring give rise to two doublets of doublets, owing to their mutual coupling and to their relatively strong ^{5}J(P,H) coupling constant of 1.5 and 3.3 Hz, respectively. The NH resonance is masked by the phenyl absorptions and could not be observed.

Similarly to the reactions leading to **5** and **6**, addition of [AuCl(THT)] to a solution of *N*-(diphenylphosphino)benzo[*d*]thiazol-2-amine (ligand **3**) gave [AuCl(**3**-κ*P*)] (**7**) in quantitative yields. Its crystal structure is shown in Fig. 4.

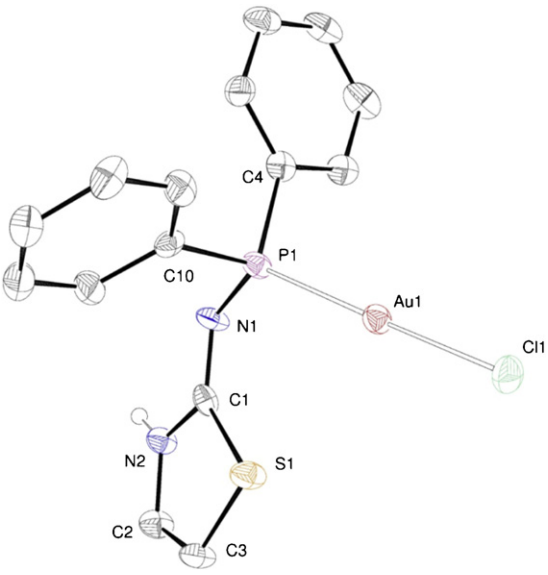

Fig. 3. ORTEP of the molecular structure of complex **6**. Ellipsoids at 40% probability level. Selected bond lengths [Å] and angles [°]: Au1–Cl(1) 2.294(4), Au1–P1 2.233(3), P1–N1 1.66(1), N1–C1 1.32(1), N1–C1 1.32(1), C1–N2 1.35(2), N2–C2 1.38(2), C2–C3 1.32(2), C3–S1 1.75(1), S1–C1 1.75(1); Cl1–Au1–P1 177.7(1), Au1–P1–N1 119.1(3), P1–N1–C1 121.1(7), N1–C1–N2 122.9(9), N1–C1–S1 129.2(8), N2–C1–S1 107.9(7).

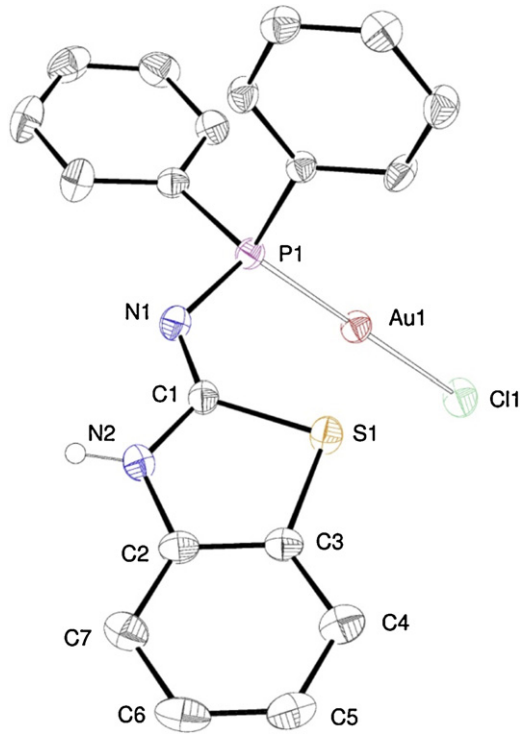

Fig. 4. ORTEP of the molecular structure of complex **7**. Ellipsoids at 40% probability level. Selected bond lengths [Å] and angles [°]: Au1–Cl(1) 2.310(1), Au1–P1 2.232(1), P1–N1 1.654(7), N1–C1 1.30(1), C1–N2 1.35(1), N2–C2 1.38(1), C2–C3 1.382(8), C3–S1 1.759(9), S1–C1 1.773(6); Cl1–Au1–P1 179.59(6), Au1–P1–N1 115.8(2), P1–N1–C1 123.2(5), N1–C1–N2 122.8(6), N1–C1–S1 128.3(5), N2–C1–S1 108.8(5).

As expected, the structure is similar to that of complexes **5** and **6**, but differently from these complexes, the formation of the H-bonded dimers is not observed. This is most likely due to the steric hindrance exerted by the benzo- group. Instead, the NH hydrogen located on the endo-cyclic N2 forms a hydrogen bond with the chlorine ligand of a neighbouring molecule. The spectroscopic data are analogous to those found in **5** and **6**.

The Au···S distance increases in the series **5**, **6**, **7** (3.034(1), 3.293(4) and 3.509(2) Å, respectively) as a result of the variation of the Au–P1–N1–C1 dihedral angle (rotation around the P–N bond). This variation indicates that no significant Au···S bonding interaction is present, since intermolecular interactions (such as the aforementioned H-bonds) overcome this hypothetical attraction.

Complexes **5** and **6** were easily deprotonated by *t*-BuOK and rapidly formed the remarkably stable dimers [Au(**1**$_{-H}$-κ*P*,κ*N*)]$_2$ (**8**) and [Au(**2**$_{-H}$-κ*P*,κ*N*)]$_2$ (**9**), respectively, via halogen cleavage and Au–N bond formation (Scheme 3). The complex [Au(**3**$_{-H}$-κ*P*,κ*N*)]$_2$ (**10**) was prepared in a one pot reaction between **3**, [AuCl(THT)] and sodium carbonate in dichloromethane. Given the rapidity of the formation of **6** under these conditions, and the lack of deprotonation when **3** was treated with Na_2CO_3, **10** is most likely formed in a stepwise reaction through deprotonation of **7**. The crystal structures of **8–10** are displayed in Figs. 5–7, respectively.

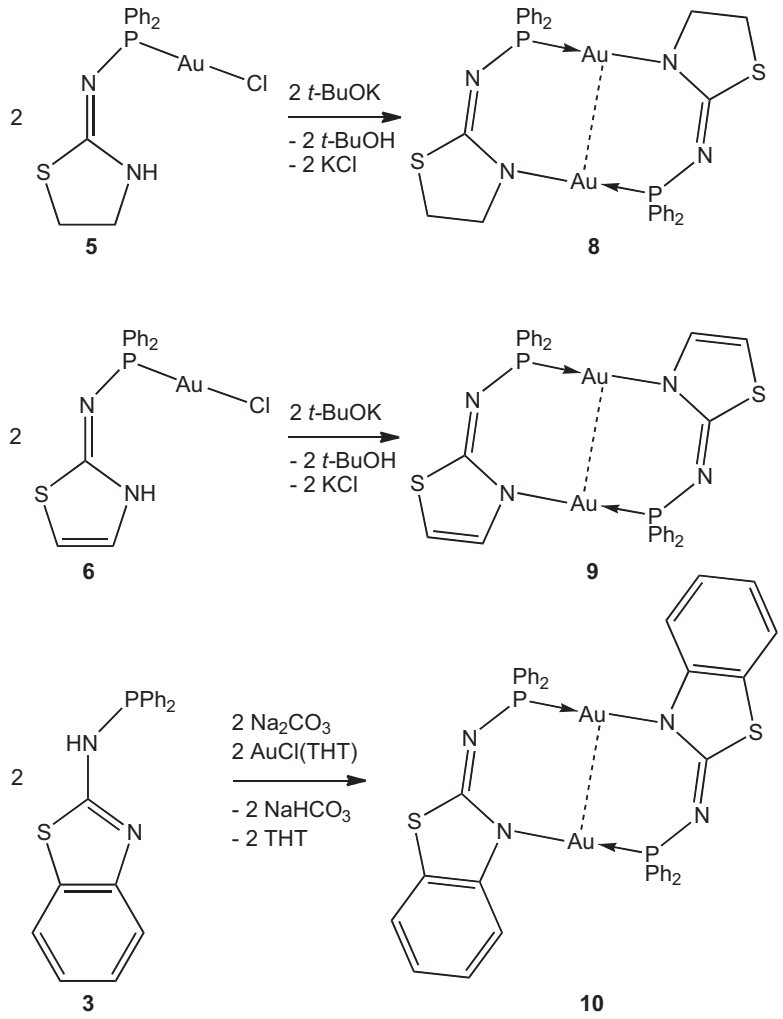

Scheme 3.

In the crystal structures of the dinuclear complexes **8**–**10**, the metal centres are doubly bridged by two deprotonated P–N ligands ($\mathbf{1}_{-H}$, $\mathbf{2}_{-H}$ and $\mathbf{3}_{-H}$, respectively), thus forming 10-membered –Au–P–N–C–N–Au–P–N–C–N– dimetallacycles**.** Each gold atom is thus coordinated, in a slightly distorted linear geometry, by a P and an N donor. A two-fold symmetry axis passes through the centroid of the two gold atoms in **8**, whereas dimers **9** and **10** show a similar, non crystallographic, approximate C_2 symmetry. In all these dinuclear complexes, the dimetallacycle is not planar. For example, in **9** (Fig. 8), the P–Au···Au–N torsion angle is 37.6(2)° and the thiazole rings main planes form an angle of 73.7(1)°.

The metal–metal separations are consistent with the presence of d^{10}–d^{10} aurophilic interactions. In Table 2, comparisons are provided between selected structural features of **8**, **9** and **10**.

The Au···Au distances range from 2.8592(4) to 2.8831(4) Å and do not vary appreciably within the series, reflecting that the differences between ligands **1**–**3** did not affect the bridging behaviour of their deprotonated forms. Interestingly, these differences were more significantly felt

Table 2
Comparison between selected structural parameters of **8**–**10**.

	8	**9**	**10**
Au···Au	2.8831(4)	2.8653(5)	2.8592(4)
Au–P	2.252(2)	2.254(2), 2.251(2)	2.250(2), 2.254(2)
Au–N	2.049(8)	2.083(6), 2.068(5)	2.084(6), 2.059(7)
P–N	1.63(1)	1.633(5), 1.635(7)	1.645(7), 1.631(7)
P–Au–N	177.3(2)	177.6(2), 174.3(4)	173.87(17), 172.86(4)
Au–P–N	121.9(4)	116.1(3), 120.3(3)	121.9(2), 122.2(3)
P–N–C	129.1(8)	130.2(6), 125.9(5)	132.7(6), 131.2(6)

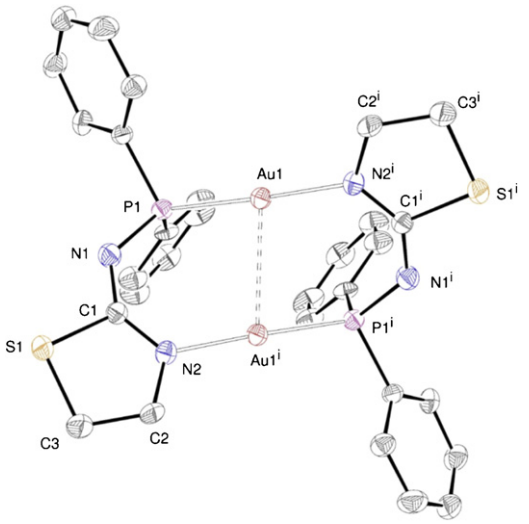

Fig. 5. ORTEP of the molecular structure of complex **8**. Ellipsoids at 40% probability level. Selected bond lengths [Å] and angles [°]: Au1···Au1^{i} 2.8831(4), Au1–P1 2.252(2), Au1–N2^{i} 2.049(8), P1–N1 1.63(1), N1–C1 1.31(1), C1–N2 1.32(1), N2–C2 1.44(1), C2–C3 1.50(2), C3–S1 1.78(1), S1–C1 1.795(9); N2^{i}–Au1–P1 177.3(2), P1–Au1···Au1^{i} 81.98(7), N2^{i}–Au1···Au1^{i} 100.5(2), Au1–P1–N1 121.9(4), P1–N1–C1 129.1(8), N1–C1–N2 134.2(9), N1–C1–S1 113.4(7), N2–C1–S1 112.4(7), Au1–N2^{i}–C1^{i} 126.9(7). Symmetry operation generating equivalent atoms (^{i}): x, –y, –z.

in the pairing by N–H···N hydrogen bonds of the complexes containing the neutral ligands (see above). These Au···Au distances compare well with those typically observed for such d^{10}–d^{10} interactions [2,3].

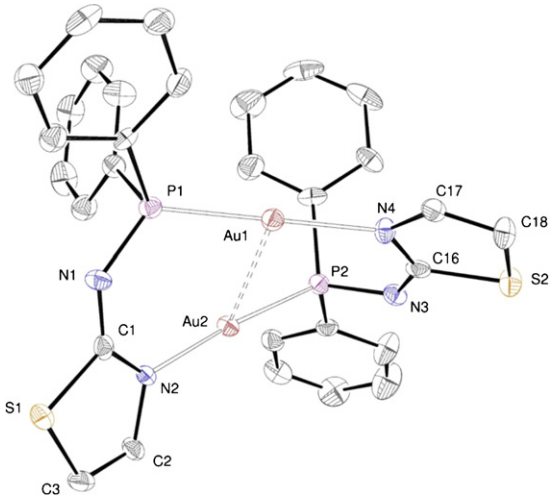

Fig. 6. ORTEP of the molecular structure of complex **9**. Ellipsoids at 40% probability level. Selected bond lengths [Å] and angles [°]: Au1···Au2 2.8653(5), P1–Au1 2.254(2), N4–Au1 2.083(6), P1–N1 1.633(5), N1–C1 1.30(1), C1–N2 1.35(1), C1–S1 1.766(6), S1–C3 1.736(9), C3–C2 1.34(1), C2–N2 1.406(7), P2–Au2 2.251(2), N2–Au2 2.068(5), P2–N3 1.635(7), N3–C16 1.32(1), C16–N4 1.34(1), C16–S2 1.760(8), S2–C18 1.73(1), C18–C17 1.33(1), C17–N4 1.40(1); P1–Au1–N4 177.6(2), P2–Au2–N2 174.3(4), P1–Au1–Au2 82.21(6), N4–Au1–Au2 99.5(2), P2–Au2–Au1 81.32(6), N2–Au2–Au1 99.6(2), Au1–P1–N1 120.3(3), P1–N1–C1 130.2(6), N1–C1–S1 117.4(6), N1–C1–N2 132.4(7), N2–C1–S1 110.2(6), C1–N2–Au2 126.8(5), Au2–P2–N3 116.1(3), P2–N3–C16 125.9(6), N3–C16–N4 131.8(7), N3–C16–S2 117.3(6), S2–C16–N4 110.9(5), C16–N4–Au1 128.2(5).

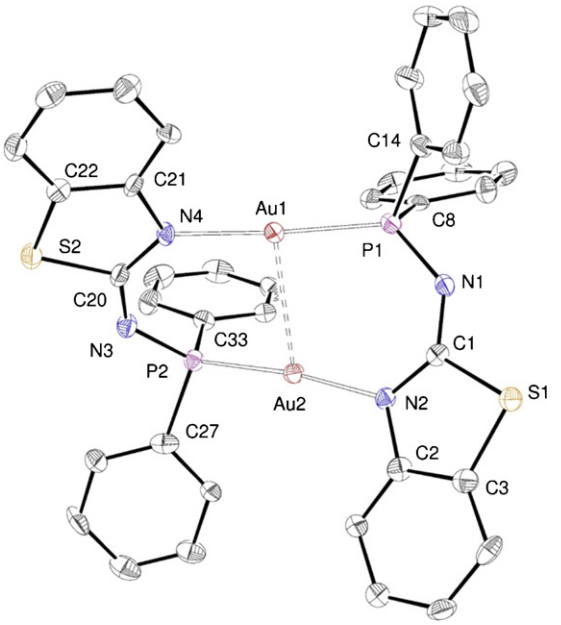

Fig. 7. ORTEP of the molecular structure of complex **10**. Ellipsoids at 40% probability level. Only one of the two, very similar, crystallographically independent molecules is shown. Selected bond lengths [Å] and angles [°]: Au1···Au2 2.8592(4), P1–Au1 2.250(2), N4–Au1 2.084(6), P1–N1 1.645(7), N1–C1 1.324(9), C1–N2 1.342(10), C1–S1 1.765(8), S1–C3 1.743(8), C3–C2 1.401(12), C2–N2 1.396(9), P2–Au2 2.254(2), N2–Au2 2.059(7), P2–N3 1.631(7), N3–C20 1.313(9), C20–N4 1.326(10), C20–S2 1.774(8), S2–C22 1.749(8), C22–C21 1.394(11), C21–N4 1.425(9); P1–Au1–N4 173.87(17), P2–Au2–N2 172.86(4), P1–Au1–Au2 85.83(5), N4–Au1–Au2 99.00(16), P2–Au2–Au1 85.65(5), N2–Au2–Au1 100.23(16), Au1–P1–N1 121.9(2), P1–N1–C1 132.7(6), N1–C1–S1 114.5(6), N1–C1–N2 132.0(8), N2–C1–S1 113.5(5), C1–N2–Au2 128.3(5), Au2–P2–N3 122.2(3), P2–N3–C20 131.2(6), N3–C20–N4 133.0(7), N3–C20–S2 114.6(6), S2–C20–N4 112.5(5), C20–N4–Au1 128.9(5).

In solution, the dinuclear structures are most likely retained. The corresponding $^{31}P\{^{1}H\}$ NMR spectra show singlets (41.0, 39.0 and 39.5 ppm for **8**, **9** and **10**, respectively), highfield shifted when compared to those of the parent mononuclear complexes. Disappearance of the NH ^{1}H NMR signal of **5** and of the ν(AuCl) IR absorption for all complexes confirmed the completeness of the reaction.

Although considerable work has been done on P,N-binucleating ligands [14], only few structures featuring

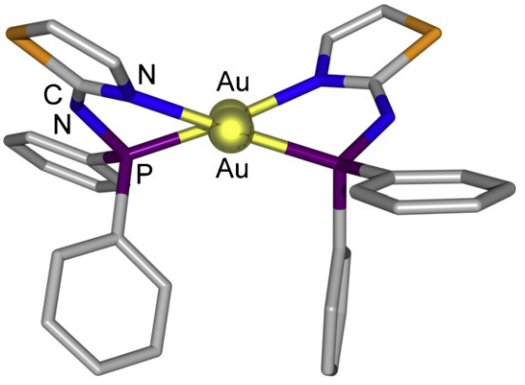

Fig. 8. View of the crystal structure of **9**.

doubly P,N-supported Au(I)–Au(I) interactions have been reported previously, featuring 10-membered [15] or eight-membered [16] metallacycles but all of these complexes were cationic, in contrast to the cases reported here. The 10-membered structures include dicationic complexes with phosphino-imine ligands displaying Au···Au distances of 2.8396(3) Å [15a] and 2.8691(4) Å [15b] and bis(2-pyridyl)phosphole complexes with Au···Au distances of 3.1232(9) and 3.1059(7) Å [15c]. The 8-membered metallacycles include digold complexes with bridging 2-pyridylphosphine ligands and a short Au. . .Au distance of 2.776(1) Å [16a], and complexes with 2-(diphenylphosphino)-1-methylimidazoles [16b] or tris(2-isopropylimidazol-4(5)yl)phosphines [16c] with Au···Au distances of 2.8174(10) and 2.8821(15) Å, respectively. Bridging P,N ligands have been also used for the assembly of trinuclear $[Au_3L_3]^{3+}$ (L = P,N bridging ligand) complexes [17].

Attempts to isolate [AuCl(**4**)], using the corresponding thiadiazole-based phosphine **4** failed, probably owing to the high sensitivity towards hydrolysis or alcoholysis of this P,N ligand. Only degradation products resulting from the cleavage of the P–N bond of **4** were observed or isolated. Thus, we were not able to isolate the related dimer $[AuCl(\mathbf{4}_{-H}\text{-}\kappa P,\kappa N)]_2$, neither in a stepwise approach nor in a one pot synthesis between **4**, [AuCl(THT)] and *t*-BuOK or Na_2CO_3.

4. Conclusions

New mononuclear gold(I) complexes **5**–**7** and dinuclear gold(I) complexes **8**–**10**, containing neutral or deprotonated thiazolines- and thiazole-based phosphine ligands, respectively, have been prepared and characterized. The anionic ligands $\mathbf{1}_{-H}$, $\mathbf{2}_{-H}$ and $\mathbf{3}_{-H}$ proved to be efficient supporting moieties, leading to stable, *neutral* dimers featuring Au(I)–Au(I) d^{10}–d^{10} interactions in the range 2.8592(4)–2.8831(4) Å. The structures of the mononuclear and dinuclear complexes have been determined by X-ray diffraction. Although the differences between ligands **1**–**3** had an influence on the pairing by N–H. . .N hydrogen bonds of the complexes containing the neutral ligands, because of steric reasons, they did not affect the bridging behaviour of their deprotonated forms and thus did not induce large variations of the Au(I)–Au(I) distances. The luminescence properties and the coordination chemistry of **8–10** will be further explored.

Acknowledgements

This work was supported by the CNRS, the *Ministère de l'Enseignement Supérieur et de la Recherche*, the Région Alsace (PhD grant to C.V.) and the *Agence Nationale de la Recherche* (ANR-06-BLAN 410).

Appendix A. Supplementary data

Supplementary data associated with this article can be found, in the online version, at doi:10.1016/j.crci.2011.09.010.

References

For recent review articles, see e.g.
[1] (a) H. Schmidbaur, A. Schier, Chem. Soc. Rev. 41 (2012), doi:10.1039/C1CS15182G;
(b) Z.N. Chen, N. Zhao, Y. Fan, J. Ni, Coord. Chem. Rev. 253 (2009) 1;
(c) A. Laguna, Modern supramolecular gold chemistry: gold-metal interactions and applications, Wiley-VCH, Weinheim, 2008;
(d) M.C. Gimeno, Modern supramolecular gold chemistry: gold-metal interactions and applications, ed. A. Laguna, Wiley-VCH, Weinheim, 2008p. 1;
(e) H. Schmidbaur, A. Schier, Chem. Soc. Rev. 37 (2008) 1931;
(f) M.J. Katz, K. Sakaib, D.B. Leznoff, Chem. Soc. Rev. 37 (2008) 1884;
(g) H. Schmidbaur, Gold. Bull. 33 (2000) 3.

and references cited therein
[2] (a) J. Muñiz, C. Wang, P. Pyykkö, Chem. Eur. J. 17 (2011) 368;
(b) P. Pyykkö, Chem. Soc. Rev. 37 (2008) 1967;
(c) P. Pyykkö, Angew. Chem. Int. Ed. 43 (2004) 4412.
[3] S. Sculfort, P. Braunstein, Chem. Soc. Rev. 40 (2011) 2741.
[4] G. Margraf, R. Pattacini, A. Messaoudi, P. Braunstein, Chem. Commun. (2006) 3098.
[5] R. Pattacini, C. Giansante, P. Ceroni, M. Maestri, P. Braunstein, Chem. Eur. J. 13 (2007) 10117.
[6] H.L. Milton, M.V. Wheatley, A.M.Z. Slawin, D.J. Woollins, Inorg. Chim. Acta 358 (2005) 1393.
[7] S. Zhang, R. Pattacini, P. Braunstein, Dalton Trans. 40 (2011) 5711.
[8] S. Zhang, R. Pattacini, P. Braunstein, Organometallics 29 (2010) 6660.
[9] R. Usón, A. Laguna, M. Laguna, Inorg. Synth. 26 (1989) 85.
[10] Bruker–Nonius, Kappa CCD Reference Manual, Nonius BV, The Netherlands, 1998.
[11] G.M. Sheldrick, Acta Crystallogr., Sect. A: Found. Crystallogr. A64 (2008) 112.
[12] N.C. Baenziger, W.E. Bennett, D.M. Soboroff, Acta Crystallogr., Sect. Sci. B32 (1976) 962.
[13] E.A. Allen, W. Wilkinson, Spectrochim. Acta 28A (1972) 2257.
[14] S. Maggini, Coord. Chem. Rev. 253 (2009) 1793–1832.
[15] (a) O. Crespo, E.J. Fernandez, M. Gil, M.C. Gimeno, P.G. Jones, A. Laguna, J.M. Lopez-de-Luzuriaga, M.E. Olmos, J. Chem. Soc., Dalton Trans. (2002) 1319;
(b) R.J. Bowen, J. Coates, E.M. Coyanis, D. Defayay, M.A. Fernandes, M. Layh, R.M. Moutloali, Inorg. Chim. Acta 362 (2009) 3172;
(c) S. Welsch, B. Nohra, E.V. Peresypkina, C. Lescop, M. Scheer, R. Réau, Chem. Eur. J. 15 (2009) 4685.
[16] (a) Y. Inoguchi, B. Milewski-Mahrla, H. Schmidbaur, Chem. Ber. 115 (1982) 3085;
(b) V.J. Catalano, S.J. Horner, Inorg. Chem. 42 (2003) 8430;
(c) P.C. Kunz, M.U. Kassack, A. Hamacher, B. Spingler, Dalton Trans. (2009) 7741.
[17] (a) U. Monkowius, M. Zabel, M. Fleck, H. Yersin, Z. Naturforsch, B. Chem. Sci. 64 (2009) 1513;
(b) C. Khin, A.S.K. Hashmi, F. Rominger, Eur. J. Inorg. Chem. (2010) 1063.